Anisotropy of Polarized X-Ray Emission from Molecules

S. H. Southworth, D. W. Lindle, R. Mayer, and P. L. Cowan[(a)]
National Institute of Standards and Technology, Gaithersburg, Maryland 20899
(Received 25 January 1991)

Strongly anisotropic, polarized Cl K-V x-ray emission from gas-phase CF_3Cl has been observed following resonant excitation with a linearly polarized x-ray beam. Distinctively different angular distributions are observed for x-ray emission involving molecular orbitals of different symmetries. A classical model of the x-ray absorption-emission process accurately describes the observed radiation patterns.

PACS numbers: 33.20.Rm

X-ray fluorescence spectrometry is widely used for quantitative chemical analysis in research and industry, and it is generally assumed that x-ray emission is isotropic [1]. The observation of anisotropic x-ray emission from molecular crystals and solids has been attributed to the inherent ordering of those samples [2], and it has been expected that randomly oriented samples, such as gas-phase molecules, will display isotropic x-ray emission. However, excitation by a photon or particle beam will generally leave an atomic or molecular target in an anisotropic state, and this anisotropy is manifested in the polarization and angular distribution of emitted photons [3,4]. We report the first observation of strongly anisotropic, polarized x-ray emission from gas-phase molecules. Specifically, the Cl 1s orbital of CF_3Cl was resonantly excited to an unoccupied valence molecular orbital (MO) using a narrow-bandwidth, linearly polarized x-ray beam, and a polarization-selective x-ray emission spectrometer was used to measure the angular dependence of the intensity of Cl K-V x-ray emission, in which a valence MO fills the Cl 1s hole. Distinctively different angular distributions are observed for Cl K-V emission involving valence MOs of different symmetries. A simple classical model accurately describes the observed anisotropies for the different MOs. This study demonstrates that the technique of polarized, angle-dependent x-ray-emission spectroscopy, following resonant photoexcitation of randomly oriented targets, provides a sensitive probe of the symmetries of the electronic states involved in the absorption and emission processes.

The experimental geometry is shown schematically in Fig. 1. Linearly polarized x rays provided by beam line X-24A [5] at the National Synchrotron Light Source were used to photoexcite CF_3Cl molecules at energies near the Cl K edge. The Cl K-V fluorescence emitted normal to the propagation direction of the incident x-ray beam was analyzed using a curved-crystal spectrometer [6]. A position-sensitive proportional counter (PSPC) [7] recorded the entire Cl K-V spectrum simultaneously. The gas cell contained 150 torr of CF_3Cl and was separated from beam-line vacuum with beryllium windows. Ionization chambers were used to measure the incident and transmitted intensities of the primary x-ray beam, providing absorption spectra and normalization for variations in beam intensity.

Si(111) crystals were used both in the beam line's double-crystal monochromator [8] and in the curved-crystal emission spectrometer [6]. For the incident x-ray energies near the Cl K edge ($E \approx 2820$–2880 eV) and for the detected Cl K-V emission ($E \approx 2800$–2820 eV) the Bragg diffraction angles are $\approx 43°$–$45°$, resulting in essentially complete suppression of the component of linear polarization having its electric vector parallel to the plane of incidence [6].

The polarization vector of the incident x-ray beam defines a natural reference axis for angular distribution studies because photoexcitation of randomly oriented targets produces an ensemble of core-excited states having cylindrical symmetry with respect to that axis [3,4]. In addition, the photoexcited system is symmetric with respect to reversal of that axis. These symmetry properties are retained in the emitted x-radiation patterns.

In order to measure angular distributions, the target chamber and emission spectrometer were mounted on a rotation platform to record x-ray spectra at different emission angles θ with respect to the polarization vector of the incident x-ray beam. The plane normal to the propagation direction of the incident x-ray beam serves as

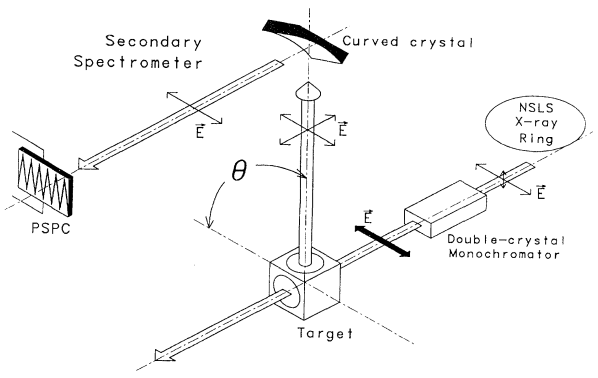

FIG. 1. Schematic diagram of the instrumentation used for the measurement of the angular distribution of polarized x-ray emission from gas-phase targets.

a reference plane for defining the observed polarization direction of the emitted x rays. The curved crystal of the emission spectrometer was positioned to transmit x rays whose polarization vectors were either parallel or perpendicular to this plane. The x-radiation patterns were characterized by two sets of measurements of the emission intensities as a function of θ. $I_{\parallel}(\theta)$ denotes the angular distribution observed for emitted x rays polarized parallel to the reference plane, and $I_{\perp}(\theta)$ denotes the angular distribution for emitted x rays polarized perpendicular to this plane.

As shown in Fig. 2, the parallel-polarized Cl K-V spectra display strong angular variations of the branching ratios for the different valence MOs when the excitation energy is tuned to a subthreshold absorption resonance assigned [9] to the Cl $1s$-to-valence transition $1a_1 \rightarrow 11a_1$. Similar variations in relative peak intensities are observed [10] at fixed emission angle ($\theta = 90°$) when parallel- and perpendicular-polarized Cl K-V spectra are compared for resonantly excited molecules.

A quantum-theoretical formulation for the polarization-dependent angular distribution of photon emission from atoms and molecules has been developed by Fano and Macek [3] and by Greene and Zare [4]. This formulation adopts a two-step model of the excitation and radiative decay. We assume here that x-ray absorption and emission may be described as electric dipole processes. The theoretical formulation relates the multipole moments of the spatial distributions of angular momenta in the initial, photoexcited, and final states of the target to the propagation directions and polarizations of the incident and emitted photons [3,4]. Photoabsorption by randomly oriented target molecules can give rise to an ensemble of excited states whose rotational angular momentum vectors are directed in space anisotropically. This excited-state anisotropy is described by an alignment parameter, and the polarization and angular distribution of the emitted photons depend on the alignment and on a geometrical factor determined by the rotational quantum numbers of the excited and final states [3,4]. In the present case, the angular distributions can be expressed by

$$I_{\parallel}(\theta) = I_0\{1 + R[3\sin^2\theta - 1]\} \quad (1)$$

and

$$I_{\perp}(\theta) = I_0\{1 - R\}, \quad (2)$$

where I_0 is proportional to the total intensity emitted in all directions and summed over polarizations, and R is the polarization anisotropy. The parameter R characterizes the radiation pattern and relates measurements to theory [11,12]. In the quantum-theoretical model [3,4], R is given by $\frac{1}{2}$ of the product of the alignment parameter and geometrical factor [11,12].

It can be seen from Eqs. (1) and (2) that the radiation patterns have simple symmetry properties. Because of the cylindrical symmetry with respect to the polarization vector of the incident x-ray beam, no dependence on azimuthal angle is expected. Also, $I_{\perp}$ is isotropic, and $I_{\parallel}(0°) = I_{\perp}$. It follows that R can be determined by measurements either of the anisotropy of the parallel component $I_{\parallel}(\theta)$ or of the polarization $P = (I_{\parallel} - I_{\perp})/(I_{\parallel} + I_{\perp})$ measured at $\theta = 90°$ as in Ref. [10].

Application of the quantum-theoretical version of the two-step model to molecular targets is complicated by the need to account for rotational transitions in absorption and emission [11]. However, while typical vacuum-ultraviolet (VUV) emission lifetimes ($\sim 10^{-8}$ s) are slow compared with rotational periods ($\sim 10^{-12}$ s), the time scale of x-ray processes ($\sim 10^{-14}$ s) is fast compared with rotational motion. This consideration brings into question the application of a two-step model to x-ray absorption and emission processes in molecules. A more accurate picture may be that of a one-step, inelastic-scattering process [13] by molecules essentially fixed in space during the time scale of the process. However, it is useful to retain the basic two-step picture in order to describe how x-ray absorption selectively excites an anisotropic distribution of target molecules and how the polarization and anisotropy of the emitted x rays depend on the symmetries of the electronic states involved.

We make use of the classical model [14,15] in which the absorption and emission dipole moments are replaced by classical dipole oscillators treated as rigidly attached to the molecular framework. The polarization and anisotropy of the emitted radiation are obtained from the

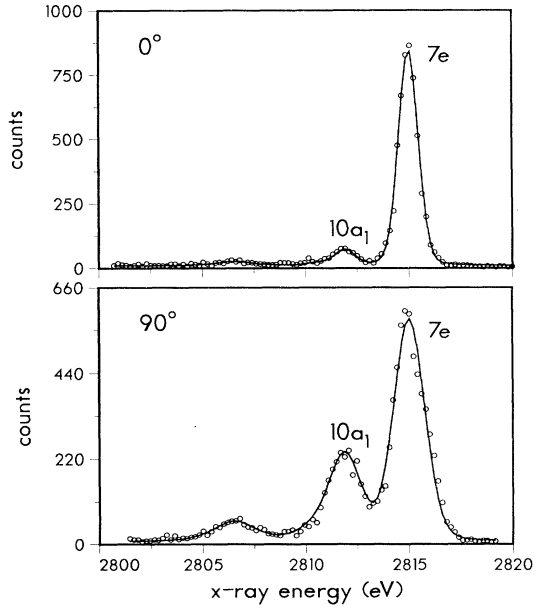

FIG. 2. Parallel-polarized Cl K-V emission spectra from CF_3Cl recorded on resonance at emission angles $\theta = 0°$ (top) and 90° (bottom). The solid curves are the results of a peak fitting procedure used to obtain emission intensities for transitions involving the $10a_1$ and $7e$ molecular orbitals.

relative directions of the absorption and emission oscillators averaged over molecular orientations. Defining γ to be the ensemble average of the angle between the absorption and emission oscillators, the polarization anisotropy is given by [15] $R=\frac{1}{5}(3\cos^2\gamma-1)$. This result can be used to predict R values for particular rotational transitions by referencing the directions of the transition dipole moments to the rotational angular momentum vectors and by taking account of the relative time scales of radiative lifetimes and rotational periods [15]. We disregard rotational motion in the present application of the classical model, treat the target molecules as fixed in space during the time scale of the x-ray absorption-emission process, and consider only the symmetries of the electronic states involved.

Applying the classical model to the $1a_1\rightarrow 11a_1$ resonant excitation of CF_3Cl, the absorption dipole moment lies parallel to the molecular figure axis (the C-Cl bond axis), and a $\cos^2\theta$ distribution of the figure axes with respect to the incident polarization vector is selectively excited. In the emission step, valence MOs having a_1 symmetry give rise to emission dipole moments also directed parallel to the figure axis, so $\gamma=0°$ and $R(a_1)=\frac{2}{5}$. MOs having e symmetry are associated with emission dipole moments directed perpendicular to the figure axis, so $\gamma=90°$ and $R(e)=-\frac{1}{5}$.

In order to compare measured angular distributions with theory, a peak fitting procedure was used to obtain the emission intensities of the transitions involving the $10a_1$ and $7e$ MOs indicated in Fig. 2. The MO assignment of the Cl K absorption and emission spectra of CF_3Cl is discussed in Ref. [9]. The collection efficiency of the emission spectrometer varied as a function of θ due to the geometry of the interaction region and due to the difficulty of maintaining precise mutual alignment of the incident x-ray beam, the gas cell, and the emission spectrometer. However, the relative collective efficiency was determined and corrected for at each θ by recording Cl K-V spectra far above ($\sim$50 eV) the Cl K-ionization threshold. Above threshold, degenerate continuum channels having a_1 and e symmetries both contribute, and the absorption dipole moment may lie parallel or perpendicular to the molecular figure axis. Only a small alignment of the core-vacancy state is expected to be produced above threshold, and the anisotropy and polarization of x-ray emission are therefore relatively weak. It has been demonstrated using VUV emission spectroscopy that measurements of the small alignments produced above threshold provide dynamical information on the photoionization of valence orbitals [11,16,17]. We anticipate that precise measurements of the polarizations and anisotropies of emitted x rays produced above threshold will provide similar information on the photoionization of core orbitals. However, in the present study we emphasize measurements of the much stronger anisotropies which result when x-ray absorption and emission involve states having well-defined symmetries. For purposes of determining the relative collection efficiency of the spectrometer, we have assumed that the x-ray emission far above threshold is essentially isotropic and unpolarized. This assumption has been confirmed to within experimental uncertainties by measurements [10] of the polarization of Cl K-V emission at $\theta=90°$. The uncertainties in the results reported here represent 1 standard deviation due to counting statistics of the x-ray spectra.

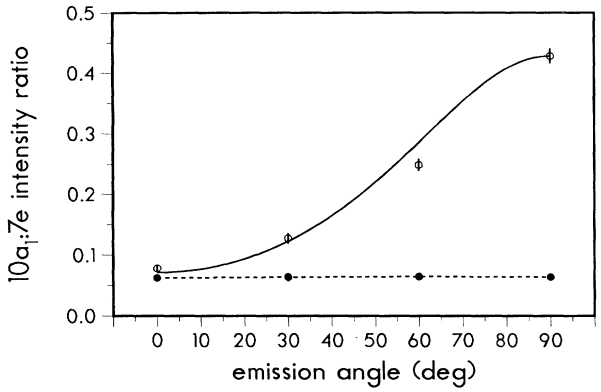

FIG. 3. Angular dependence of the $10a_1$:$7e$ emission intensity ratio measured using parallel polarization (○) and perpendicular polarization (●). The solid curve is a theoretical prediction for parallel polarization based on a classical model and has been normalized to the measurement at $\theta=90°$. The dashed curve simply connects the results measured using perpendicular polarization.

Using the classical values for $R(a_1)$ and $R(e)$ in Eqs. (1) and (2) and normalizing to the perpendicular component ($I_\perp=1$) in each case, the predicted anisotropies of the parallel components are $I_\parallel(a_1)=1+2\sin^2\theta$ and $I_\parallel(e)=\frac{1}{2}(1+\cos^2\theta)$. The measured values of $I_\parallel(90°)/I_\parallel(0°)$ are 2.7 ± 0.2 and 0.50 ± 0.02 for the $10a_1$ and $7e$ MOs, respectively, in good agreement with the classical-model predictions of 3 and $\frac{1}{2}$. For the perpendicular components, which should be isotropic, we obtained $I_\perp(90°)/I_\perp(0°)=0.90\pm0.10$ and 0.88 ± 0.05 for the $10a_1$ and $7e$ MOs, respectively. In Fig. 3 the $10a_1$:$7e$ intensity ratios are plotted for both parallel- and perpendicular-polarized measurements. Also plotted is the intensity ratio for parallel polarization predicted by the classical model and normalized to the measured ratio at $\theta=90°$. While the perpendicular-polarized intensity ratio is isotropic, as expected, the parallel-polarized intensity ratio varies by a factor of 6. This comparison demonstrates the distinct difference in the radiation patterns for the two MO symmetries. The simple classical model is in fairly good quantitative agreement with the observed anisotropies.

Finally, the determination of total intensities I_0 is of interest in many applications of x-ray emission spectrometry. For the present study, Eq. (1) shows that an intensity proportional to I_0 is given by $I_\parallel$ at the "magic angle," $\theta_m=\sin^{-1}(3^{-1/2})\approx 35.3°$. For example, the

resonant oscillator-strength ratio for the $10a_1$ and $7e$ transitions is given by the parallel-polarized $10a_1$:$7e$ intensity ratio at θ_m. Using the measurements and theoretical curve plotted in Fig. 3, we obtain $I_0(10a_1):I_0(7e) = 0.14 \pm 0.01$.

We thank R. D. Deslattes for contributions to the design of this experiment, and we thank B. A. Karlin for assistance in performing the measurements. The measurements were made at the National Synchrotron Light Source, Brookhaven National Laboratory, which is supported by the U.S. Department of Energy, Division of Materials Sciences and Division of Chemical Sciences.

---

[a]Present address: Argonne National Laboratory, Argonne, IL 60439.

[1] R. Jenkins, *X-Ray Fluorescence Spectrometry* (Wiley, New York, 1988); C. J. Sparks, Jr., in *Synchrotron Radiation Research,* edited by H. Winick and S. Doniach (Plenum, New York, 1980), pp. 459–512.

[2] A. Faessler, E. Gilberg, and G. Wiech, in *Advances in X-Ray Spectroscopy,* edited by C. Bonnelle and C. Mandé (Pergamon, New York, 1982), pp. 210–224.

[3] U. Fano and J. H. Macek, Rev. Mod. Phys. **45**, 553 (1973).

[4] C. H. Greene and R. N. Zare, Annu. Rev. Phys. Chem. **33**, 119 (1982).

[5] P. L. Cowan, S. Brennan, R. D. Deslattes, A. Henins, T. Jach, and E. G. Kessler, Nucl. Instrum. Methods Phys. Res., Sect. A **246**, 154 (1986); P. L. Cowan, S. Brennan, T. Jach, D. W. Lindle, and B. A. Karlin, Rev. Sci. Instrum. **60**, 1603 (1989).

[6] S. Brennan, P. L. Cowan, R. D. Deslattes, A. Henins, D. W. Lindle, and B. A. Karlin, Rev. Sci. Instrum. **60**, 2243 (1989).

[7] B. P. Duval, J. Barth, R. D. Deslattes, A. Henins, and G. G. Luther, Nucl. Instrum. Methods **222**, 274 (1984).

[8] P. L. Cowan, J. B. Hastings, T. Jach, and J. P. Kirkland, Nucl. Instrum. Methods **208**, 349 (1983).

[9] R. C. C. Perera, P. L. Cowan, D. W. Lindle, R. E. LaVilla, T. Jach, and R. D. Deslattes, Phys. Rev. A **43**, 3609 (1991).

[10] D. W. Lindle, P. L. Cowan, R. E. LaVilla, T. Jach, R. D. Deslattes, B. Karlin, J. A. Sheehy, T. J. Gil, and P. W. Langhoff, Phys. Rev. Lett. **60**, 1010 (1988); D. W. Lindle, P. L. Cowan, R. E. LaVilla, T. Jach, R. D. Deslattes, R. C. C. Perera, and B. Karlin, J. Phys. C **9**, 761 (1987); D. W. Lindle, P. L. Cowan, T. Jach, R. E. LaVilla, R. D. Deslattes, and R. C. C. Perera, Phys. Rev. A **43**, 2353 (1991).

[11] J. A. Guest, K. H. Jackson, and R. N. Zare, Phys. Rev. A **28**, 2217 (1983).

[12] S. H. Southworth, D. W. Lindle, R. Mayer, and P. L. Cowan, Nucl. Instrum. Methods Phys. Res., Sect. B **56/57**, 304 (1991).

[13] T. Åberg and J. Tulkki, in *Atomic Inner-Shell Physics,* edited by B. Crasemann (Plenum, New York, 1985), pp. 419–463.

[14] P. P. Feofilov, *The Physical Basis of Polarized Emission* (Consultants Bureau, New York, 1961).

[15] R. N. Zare, *Angular Momentum* (Wiley, New York, 1988).

[16] C. D. Caldwell and R. N. Zare, Phys. Rev. A **16**, 255 (1977).

[17] E. D. Poliakoff, J. L. Dehmer, D. Dill, A. C. Parr, K. H. Jackson, and R. N. Zare, Phys. Rev. Lett. **46**, 907 (1981).